# 行政院國家科學委員會專題研究計畫 成果報告

## RFID 系統發展及其產業應用--總計畫：RFID 系統發展及其產業應用(3/3)

## 研究成果報告(完整版)

計 畫 類 別 ：整合型
計 畫 編 號 ：NSC 95-2218-E-002-006-
執 行 期 間 ：95 年 08 月 01 日至 96 年 07 月 31 日
執 行 單 位 ：國立臺灣大學機械工程學系暨研究所

計 畫 主 持 人 ：黃漢邦
共 同 主 持 人 ：吳文中、郭瑞祥、陳凱瀛
計畫參與人員：碩士班研究生-兼任助理：金威翰、陳育章、鄭哲欣、白宗正
共同主持人：吳文中、陳凱瀛、郭瑞祥

處 理 方 式 ：本計畫可公開查詢

中 華 民 國 96 年 12 月 04 日

# 行政院國家科學委員會補助專題研究計畫成果報告

## RFID 系統發展及其產業應用

計畫類別：□個別型計畫　　☑整合型計畫
計畫編號：NSC 95-2218-E-002-006
執行期間：95 年 8 月 1 日至 96 年 7 月 31 日


主持人：黃漢邦　台灣大學機械工程學系
共同主持人：吳文中　台灣大學工程科學與海洋工程學系
共同主持人：陳凱瀛　台北科技大學工業工程與管理系
共同主持人：郭瑞祥　台灣大學工商管理學系


本成果報告包括以下應繳交之附件：
□赴國外出差或研習心得報告一份
□赴大陸地區出差或研習心得報告一份
□出席國際學術會議心得報告及發表之論文各一份
□國際合作研究計畫國外研究報告書一份

執行單位：

中　華　民　國　96 年　　7 月　31 日

# 行政院國家科學委員會專題研究計畫成果報告

## RFID 系統發展及其產業應用

## Development of RFID System and Its Application to Semiconductor Industry

計畫編號：NSC 95-2218-E-002-006

執行期限：95 年 8 月 1 日至 96 年 7 月 31 日

主持人：黃漢邦 台灣大學機械工程學系

共同主持人：吳文中 台灣大學工程科學與海洋工程學系

共同主持人：陳凱瀛 台北科技大學工業工程與管理系

共同主持人：郭瑞祥 台灣大學工商管理學系

研究人員：

金威翰、陳育章 台灣大學工業工程研究所

鄭哲欣、白宗正 台灣大學工業工程研究所

**一、中文摘要**

RFID 技術是一種電子式的資訊承載裝置，主要是利用射頻訊號以無線通訊的方式來傳輸資料，具備遠距讀取、高儲存量等特性，被視為取代傳統條碼的新興技術，並可用於辨別、追蹤、排序和確認各式各樣的物件，相當適合應用在門禁管理、車輛辨識、資產追蹤、存貨控制、動物晶片、與工廠自動化。本計畫主要的目標是將 RFID 的技術應用於半導體產業，並針對 RFID 晶片、RFID 系統軟體環境、RFID 應用在工廠內部維修診斷、及 RFID 應用在工廠外部的供應鏈管理作一完整探討。

子計畫一的目標主要有三大項，首先是無線辨識系統標籤的天線與晶片之設計與製作；其次是奈米碳管電晶體開發；最後是有機薄膜電晶體之製程開發。在過去三年中，已建構完整全噴墨有機薄膜電晶體製程，除建構完善的噴墨系統外，並以製程改進改善有機薄膜電晶體的電性，並成功的製作簡單的反向器電路，未來將朝向製作全噴墨的完整 RFID 晶片努力。

子計畫二擬進行三大研究議題：(1)建立以 RFID 為基礎之製造系統資訊收集平台。(2)建立以 RFID 為基礎之製造系統單元控制器。(3)發展以 RFID 為基礎之在製品管制追蹤(WIP Tracking)控制機制。第三年重點為在第一年已經建置以 RFID 為主之彈性製造單元上發展生產線管理之應用。已完成之具體工作成果為(1) 在台北科技大學建置完成以 RFID 為主之彈性製造系統。(2)測試將生產控制所需在製品完全寫入 RFID 標籤中(3)測試與智慧型推論系統之整合。(4)發展 PDA 與彈性製造系統結合之應用。

子計畫三主要發展一個以無線射頻識別(RFID)為基礎的智慧型遠端診斷及維修系統，包括：(1) 第一年-整合 RFID 技術與使用嵌入式 WinCE .NET 為作業系統之 PDA 元件，融入多感測器融合技術及設計資料發送/接收器之配置;(2) 第二年-智慧型遠端診斷維修系統之發展;(3) 第三年-知識管理系統的發展。

透過第二年所建置的智慧型遠端診斷維修系統，利用 RFID 技術為基的製造系統，整合多種資料探勘方法建構即時重排程系統及決策支援系統。

子計畫四旨在以半導體產業為研究平台進行三大研究議題：(1)建立以 SCOR 與 RFID 為基礎之供應鏈績效監督指標；(2)建構描述供應鏈行為的監督模式；(3)發展以 RFID 為基礎的控制機制。第三年的重點在於結合 RFID 所提供的資訊與第二年所提出的層級監督模式，發展以前端為基礎之半導體供應鏈監控模式。已完成之具體的工作成果分為(1)建構以前端為主之二層級監控模式；(2) 發展 CONWIP 控制方式與模式求解；(3)設計模擬情境與進行模式比較。

經由模式驗證結果可有下列結論：本研究以層級在製存貨取代階段在製存貨作為監控上界，使整體供應鏈系統於在製存貨量較低的情況下同時具有較佳的服務水準。

**關鍵詞**：電子標籤、塑膠晶片、奈米碳管電晶體、有機薄膜電晶體、無線射頻辨識、單元控制器、在製品管制追蹤、智慧型決策支援系統、個人數位助理、診斷、知識管理、派工法則、決策支援、半導體供應鏈、監控機制、層級在製存貨。

**Abstract**

This project intends to develop the RIFD tag, the RFID system integration environment, the RFID-based maintenance and diagnostics, and the RFID-based supply chain monitoring and control. Then, the system will be applied to semiconductor industry.

In subproject 1, there are 3 major parts. For the first year, the antenna design and optimization process for HF and UHF tags are developed. For the second part, the process of carbon nanotube field effect transistor (CNFET) was tried out for a possibility to fabricate plastic RFID chips. Finally, the target is the process thin-film-field effect transistor. For the third part, an all ink-jet printed organic thin film transistors (OTFT) process was developed. A complete homemade ink-jet printing system was completed, and with process improvement, the performance of OTFT is in feasible stage. A simple logic inverter circuit was successfully demonstrated, and toward the goal to fabricate all printed RFID chip in near future.

The goals of subproject 2 are to: (1) design information infrastructure for RFID based manufacturing systems; (2) develop a cell controller for RFID based manufacturing systems; and (3) develop an RFID based WIP tracking model. In the third year, we have completed four major tasks: (1) Establish an RFID based flexible manufacturing system. (2) Control FMS based on WIP data written on RFID tags. (3) Integrate with Intelligent Decision Support System. (4) Develop PDA application with FMS.

Subproject 3 aims to develop an intelligent remote diagnosis and maintenance system which is based on the brand-new technology RFID including: (1) the first year - combine RFID technology with PDA (embedded WinCE .NET operating system) using the multi-sensor fusion algorithm and design the allocation of the transmitter and receiver of RFID; (2) develop of the intelligent remote diagnosis and maintenance system in the second year; (3) the third year - construct the knowledge management system.

Through the intelligent remote system constructed in the second year, RFID technology and various data mining methods are integrated to construct the on-line rescheduling system and the decision support system for manufacturing environment.

In subproject 4, the goals of this three-year research are to: (1) design SCOR-based and RFID-based supply chain performance monitoring metrics, (2) construct a RFID-based supply chain monitoring model, and (3) develop RFID-based control schemes. In the third year, we have completed three major tasks: (1) construct a forward echelon-based monitoring model, (2) develop CONWIP control method and solution procedures, and (3) design scenarios and conduct simulations to compare the performance of different control schemes.

Based on the validation results, we conclude that the proposed control scheme obtains a higher service performance compared to the traditional method.

**Keywords**: RFID, plastic electronics, organic thin-film-transistors (OTFT), carbon nanotube field effect transistor (CNT-FET), Cell Controller, WIP Tracking, Intelligent Decision Support System, PDA Diagnosis, Knowledge Management, Dispatching Rules, Decision Supporting Semiconductor Supply Chain, Monitoring & Control, Echelon WIP Inventory.

## 二、緣由與目的

RFID is the electronic device stored tremendous information. The signal of RFID is delivered through wireless communication. Because of its huge storage, remote data accessing, and non-contact reading, the traditional barcode will be replaced with brand –new RFID technology. RFID can be applied to security management, automobile identification, logistic control, biochip, and manufacturing automation, etc. This project intends to develop the RIFD tag, the RFID system integration environment, the RFID-based maintenance and diagnostics, and the RFID-based supply chain monitoring and control. Then, the system will be applied to semiconductor industry.

Since our purpose is to: (1) design information infrastructure for RFID based manufacturing systems; (2) develop a cell controller for RFID based manufacturing systems; and (3) develop an RFID based WIP tracking model. In the third year, we have completed several major tasks:

Objective 1: A complete homemade ink-jet printing system was completed, and with process improvement, the performance of OTFT is in feasible stage. A simple logic inverter circuit was successfully demonstrated, and toward the goal to fabricate all printed RFID chip in near future.

Objective 2: (1) Establish an RFID based flexible manufacturing system. (2) Control FMS based on WIP data written on RFID tags. (3) Integrate with Intelligent Decision Support System. (4) Develop PDA application with FMS.

Objective 3: RFID technology and various data mining methods are integrated to construct the on-line rescheduling system and the decision support system for manufacturing environment.

Objective 4: (1) construct a forward echelon-based monitoring model, (2) develop CONWIP control method and solution procedures, and (3) design scenarios and conduct simulations to compare the performance of different control schemes.

## 三、研究方法

### 3.1 Subproject 1: Develop of RFID tags using plastic electronic technology

#### 3.1.1 Accomplishment 1: Antenna Design for RFID Tags

The achievement is as same as before. The impedance and the gain of optimized antennas are better than original design one. From the results of this second optimization, we found that antenna performance is better than before.

#### 3.1.2 Accomplishment 2: Carbon Nanotube Field Effect Transistor Process Development

According to the measurement, we could deduce that carbon nanotubes include single-walled

carbon nanotubes (SWNT) and multi-walled carbon nanotubes (MWNT). Secondly, we measure the curve of current and voltage. When gate voltage is less than 4V, the channel began to form and the transistor turned on in Fig.1(a). If the gate voltage increases, the current of drain-source will be bigger, in Fig.1. Besides, the operative current is about several micro ampere and the off current is less than 1 nano ampere, the on/off ration is about $10^{4.}$ According the measurement and principle, we can deduce the carbon nanotube flied effect transistors (CNFETs) are p-type CNFETs. In the future, we will try to transfer our CNT-FET to the PI layer.

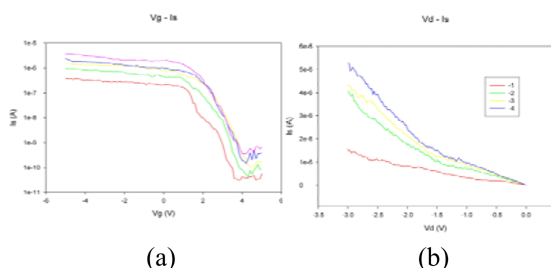


(a) (b)

Figure 1 I-V curve of CNFET

### 3.1.3 Accomplishment 3: All Ink-jet Printed Plastic Electronics

In this study, we focus on the development and improvement of the all ink-jet printed process for better electrical performance on fabricating OTFT. The homemade ink-jet printing system is shown in Fig 2(a), and the droplet formation cycle of taken is shown in Fig. 2(b). The system comprise of a drop-on-demand printhead, a back pressure controller, a ink reservoir, 2 axes motorized positioning stages, printhead driving electronics, and a droplet imaging system. The whole system is controlled by a PC running a control program developed with LabVIEW. The drop-on-demand piezoelectric driving printhead is manufactured by MiroFab Co. Ltd, and the model name is MJ-ATP®, which is designed for working in room temperature with low viscosity (<20cPs). A two-axes motorize stage system with a CCD camera are combined for the precision positioning and also the alignment for different printing layers. Another CCD camera with synchronized LED illumination with the printhead driving waveform are used as a stroboscope to monitoring the cycle of droplet formation and ensure the stability and reliability of the printing process.

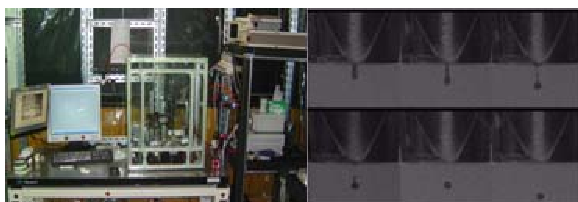

Figure 2 (a) The homemade ink-jet printing platform (b) The formation of the droplet taken by imaging system.

The bottom gate and bottom contact structure was chosen for the all ink-printed OTFT fabrication. Heat-resistant and chemistry-resistant polyimide (PI) tape is chosen as the flexible substrate. When sticking on a glass plate the roughness of the PI layer can be around 10nm, and that would be important for the OTFT device structure fabrication. The material of the gate electrode is 20% conducting polymer poly(3,4- ethylenedioxythiophene) / poly (styrenesulfonate) (PEDOT/PSS) aqueous dispersion dissolved in water, and 1% ethylene glycol (EG) are added to enhance the conductivity in around 100 S/cm. The viscosity and contact angel of the solution between substrate were 2.46cP and 56°, respectively. The Orifice diameter of printhead used on gate electrode printing is 30μm, which can achieve printing resolution in around 10μm. Single line pattern is printed as the gate electrode to reduce the parasitic capacitance of the device, and the width is 100μm with 2500 droplets per $mm^2$. The gate electrode is then baked for 1 hour in 100°C to improve the chemistry -resistance of the conducting film. The material for the insulation layer is 3.5% poly (vinylphenol) (PVP) and 0.35% cross-link agent poly (melamine-co-formaldehyde) (PMF) dissolved in hexanol. The viscosity and contact angel of the solution between substrate are 8.8cP and 10°, respectively. The Orifice diameter of printhead used for insulation layer printing is 80μm. A squared shaped pattern, 800μm by 800μm, is printed as the insulation layer. For better insulation, two layers of PVP are printed and the droplets density is around 500 droplets per 500mm, and the thickness is around 700nm. The PVP layer is then baked at 200°C for 10min for solvent evaporation and cross-linking of PVP. The same PEDOT/PSS solution as the gate electrode is used to print drain and source electrode as well. Two parallel lines are printed as drain and source electrodes. The fine spacing between the two parallel lines has to be well controlled for narrower channel length. The best resolution printed with the 30μm orifice is around 10μm. Thus, the channel area between the two printed electrodes is 20μm and channel width is 400μm controlled by the length of parallel lines. The organic semiconductor active material is 98.5% high regioregularity poly (3-hexylthiophene) (rr-P3HT) purchased from Sigma-Aldrich, and *p*-xylene is chosen over volatile chloroform as solvent to prevent clogging of printhead. However, P3HT shows poor solubility in *p*-xylene and was always precipitated around the reservoir in room temperature, and then cause failure of the printing process. To resolve this problem, a heated reservoir is used while printing P3HT. Higher temperature does prevent the precipitation of P3HT in *p*-xylene, and also help for better film formation. Moreover, the organic semiconductor active layer for forming the conducting channel is only several nm above the insulator, and thus thinker layer will not help for the field effect but degrade the off-current by leakage between drain and source electrodes. Reducing the

concentration of P3HT dissolved in *p*-xylene is the most efficient way to lower the thickness of the printed film of P3HT. The well controlled lowest concentration while forming a complete film is 0.15% with reservoir heated to 45°C. The orifice of printhead used for printing active layer is also 30µm. The viscosity and contact angel of the solution between the insulation layer is 0.7cP and 8.7°, respectively. The thickness of the printed active layer is about 25nm with the drop density of 155 droplets per $mm^2$. The printed P3HT layer is then baked 70℃ for 1 hour in vacuum to avoid the solvent remain in the film which may degrade performance of the device. The complete ink-jet printing process is shown in Fig 3(a) and the picture of printed OTFT is shown in Fig 3(b).

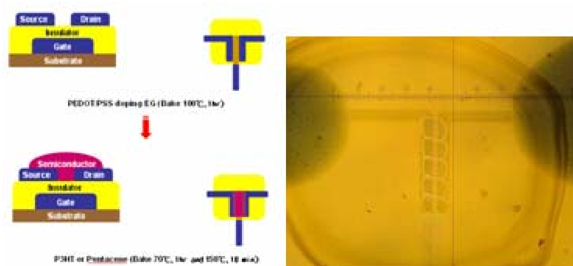

Figure 3 (a) The OTFT printing process. (b) The photo of the OTFT printed.

In addition, due to high moisture and oxygen sensitivity of P3HT, the off current will dramatically increase when the device is measured in ambient environment. The poor on/off ratio smaller than 10 was measured in such condition. To avoid that, the device is protected with another PI layer, and bakes at 60°C for 5min to remove the solvent, but not destroyed the underlying structure. The PI passivation will lower the permeability of water vapor and oxygen to P3HT, and much more improve the performance of OTFT. The electrical characteristics of OTFT printed was measured by Keithley 4200 in ambient environment. The measurement results is showed in Fig 4 (a) and Fig4 (b) for device with PI passivation

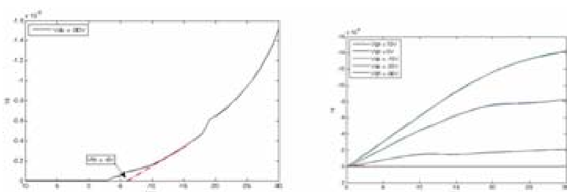
Figure 4 Measured OTFT (a) transfer characteristic and (b) output characteristics

The field-effect mobility in the saturation region was calculated from

$$I_D = \frac{1}{2}\mu C_i \frac{W}{L}\left(V_G - V_T\right)^2 \qquad \text{Eq. 1}$$

,where $I_D$ is the drain current density, μ is the field-effect electron mobility, $C_i$ is the capacitance per unit area of insulation layer ($C_i$ = 70nF/$mm^2$ were measured using Agilent 4294 impedance analyzer), W and L are channel width and length respectively (W/L = 20 here), and $V_G$ and $V_T$ are gate and threshold voltage and can be derived from the transfer characteristics. The highest field-effect mobility measured is .11 $cm^2$/V s, the threshold voltage is -6V, the on/off ratio is $1.2\times10^4$ and the subthreshold slop is -8 V/dec. A simple logic inverter circuit with 2 printed OTFT and printed resistors and capacitors are also successfully fabricated, and the input/output voltage waveform is shown in Fig. 5

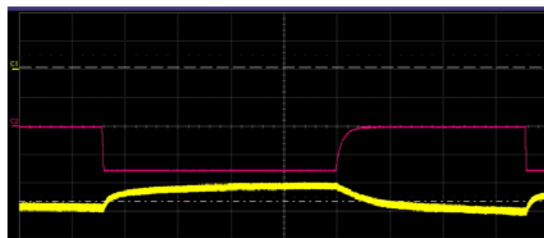
Figure 5 The input/output voltage waveform of the logic inverter circuit.

In summary, the printed OTFT has superior performance when PI is used as passivation to protect the device and with thinner semiconductor active layers. The OTFT fabricated can have low threshold voltage, high on/off ratio, and also high electron mobility. This work shows the excellent potential of ink-jet printing process for low-cost printed flexible electronics.

### 3.2 Subproject 2: Research of developing information infrastructure and application for RFID based manufacturing systems

#### 3.2.1 Accomplishment 1: Establish an RFID based flexible manufacturing system.

We have established an RFID-based FMS in the MES Lab of National Taipei University of Technology. This FMS consists of four virtual equipments, one loading station, one RGV, one unloading robot (ABB IRB 2000) and nine buffer stations. Omron passive tag (530KHz, 254 Bytes) is attached in each pallet and each pallet contains four workpieces (as shown in Figure 6). In this system, the updated status of pallet is written to pallet's tag by means of reader when the operation is completed in each virtual equipment. When workpiece finish all its operation steps and pallet is moved to unloading station, the robot will pick each workpiece to its position according to the tag content written in previous operation steps.

Figure 6 RFID based FMS in NTUT

### 3.2.2 Accomplishment 2: Control FMS based on WIP data written on RFID tags.

In the second year, we have constructed modular Colored Petri Models for equipment (CNC), material handling system (mobile robot), Loading station, unloading machine and RFID reader. In the third year, we attempt to write attributes (color of places) of CPN model into RFID tags. The updated status of pallet (i.e. colored token of CPN model) is written to pallet's tag by means of reader when the operation is completed in each virtual equipment. The content of colored tokens of CPN model and related RFID tag content are listed as shown in Table 1. Some reading and writing screens shown in monitor screen of cell controller are shown in Figure 7-8.

Table 1. CPN colored token vs. RFID tag content

| Byte | Pos. | Attr. | Value | Content | No. of bytes |
|---|---|---|---|---|---|
| 3 | 0~2 | a | 000 ~ 999 | Pallet No. | 3 |
| 6 | 3~5 | b | 000 ~ 999 | Part No. | 3 |
| 9 | 6~8 | c | 000 ~ 999 | Total no. of Op | 3 |
| 12 | 9~11 | d | 000 ~ 999 | Now op seq. | 3 |
| 16 | 12~15 | e | P000 ~ P999 | Process No. | 4 |
| 17 | 16 | f | H or N | Pallet Status | 1 |
| 20 | 17~19 | g | 000 ~ 999 | Pallet Position | 3 |
| 23 | 20~22 | h | 000 ~ 999 | Pallet new pos. | 3 |
| 24 | 23 | i | Y or N | Move Y/N | 1 |
| 29 | 24~28 | j | Ex:CNC01 | Equipment Name | 5 |
| 32 | 29~31 | k | 000 ~ 999 | Equipment No. | 3 |
| 38 | 32~37 | l | Form: hhmmss | Start time | 6 |
| 44 | 38~43 | m | Form: hhmmss | Finish time | 6 |
| 50 | 44~49 | n | Form: hhmmss | Accu. wait time | 6 |
| 56 | 50~55 | o | Form: hhmmss | Accu. Mach. time | 6 |
| 64 | 56~63 | p | Ex:1A2B3C4D | Workpiece level | 8 |

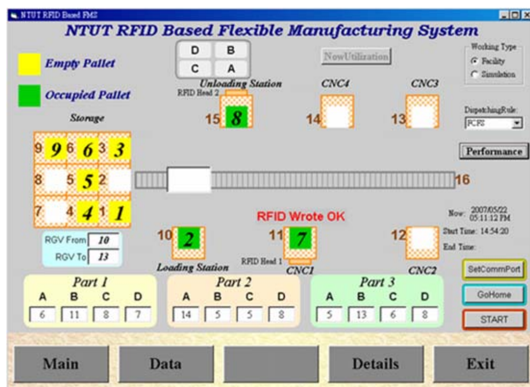


Figure 7 RFID writing status

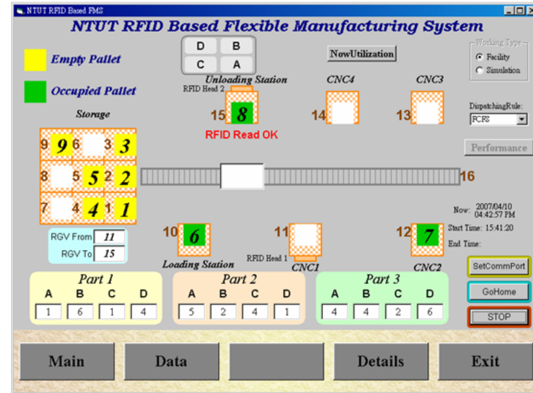


Figure 8

### 3.2.3 Accomplishment 3: Integrate with Intelligent Decision Support System.

We have integrated our RFID based FMS with Intelligent Decision Support Sytsem (IDSS), developed by ITRI. Cell controller sends all shop floor status to IDSS, and IDSS feedbacks inferring results (i.e. RGV from to command) to cell controller. IDSS runs over JESS (Java Expert System Shell) which is a rule engine and scripting environment written entirely in Sun's Java$^{TM}$ language. The JESS shell provides the basic elements of an expert system which includes a fact-list which provides a template for both knowledge and application, a knowledge base that contains all the rules and an inference engine which controls overall execution of rules. The interaction between FMS cell controller and IDSS is shown in Figure 9.

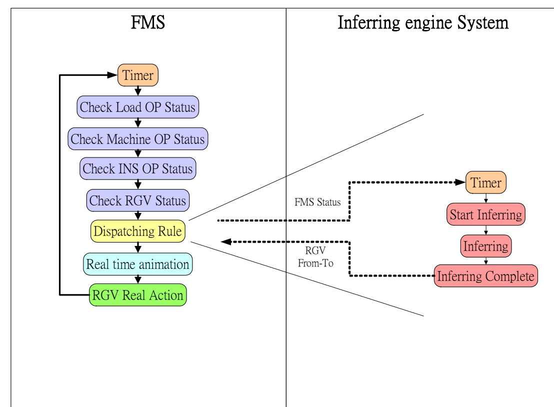


Figure 9 Interaction between FMS and IDSS

We also compare the performance of FMS with FMS+IDSS. It is shown in Figure 10. By this figure, we find that the machine utilization based on dispatching by our cell controller is better than dispatching by IDSS. This is because the communication and handshaking between cell controller and IDSS cause time lag that may miss the time of optimal decision.

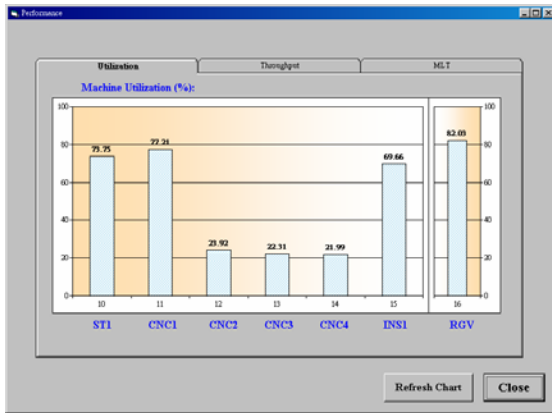


Figure 10(a)  Machine utilization of FMS

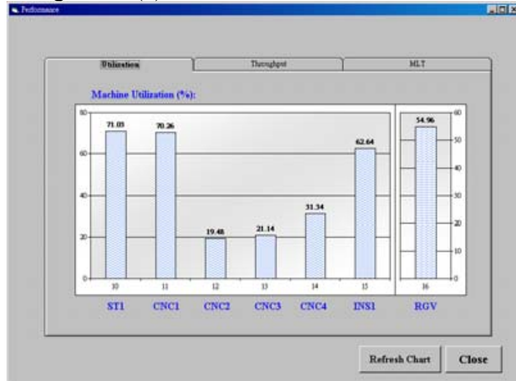


Figure 10(b)  Machine utilization of FMS+IDSS

### 3.2.4 Accomplishment 4: Develop PDA application with FMS.

We have developed PDA applications with FMS. There are two scenarios deployed in our RFID based FMS. One scenario is if number of grade C of finished goods produced in FMS greater than a predefined number, there will have a message automatically generated by cell controller and appears in supervisor's PDA. Another scenario is when count of operation of specific equipment greater than a predefined number, there will cause the equipment stopping operation and a message will be automatically generated by cell controller and appears in supervisor's PDA. When some actions have been finished and specific button on monitor screen is pressed, the equipment will start to operation again. The screens displayed in PDA and monitor screen are shown in Figure 11 and 12 respectively.

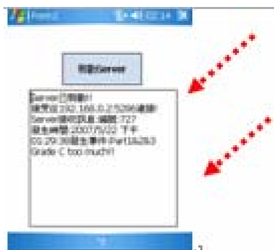

Figure 11(a)  PDA snapshot of scenario 1

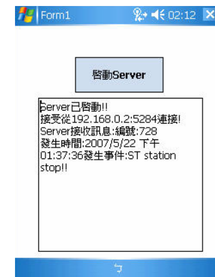


Figure 11(b)  PDA snapshot of scenario 2

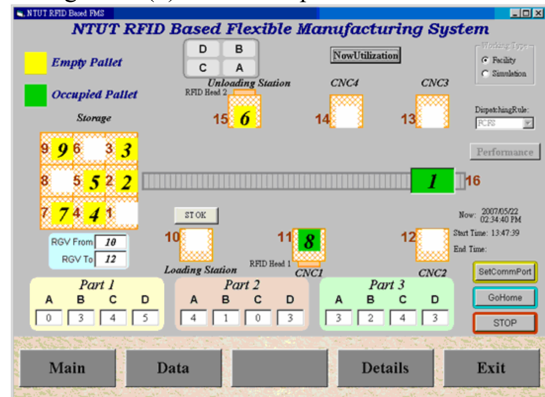


Figure 12  Monitor screen of cell controller

## 3.3 Subproject 3: RFID-based diagnosis and maintenance system

### 3.3.1 Accomplishment 1: On-Line Sceduling

The illustration for the interval variant rescheduling is shown in Figure 13. A long run of the fab consists of several decision points. Between two decision points, it contains some scheduling intervals (SI). The length of the scheduling intervals may differ in different two decision points. At each decision point, the interval variant rescheduling mechanism decides the new scheduling intervals for this decision period with the constructed ANFIS models. And at the beginning of a scheduling interval, the interval variant rescheduling mechanism determines a dispatching rule set for all machines with the constructed SVM models.

The detailed procedures for building the SVM model and ANFIS model are coming next.

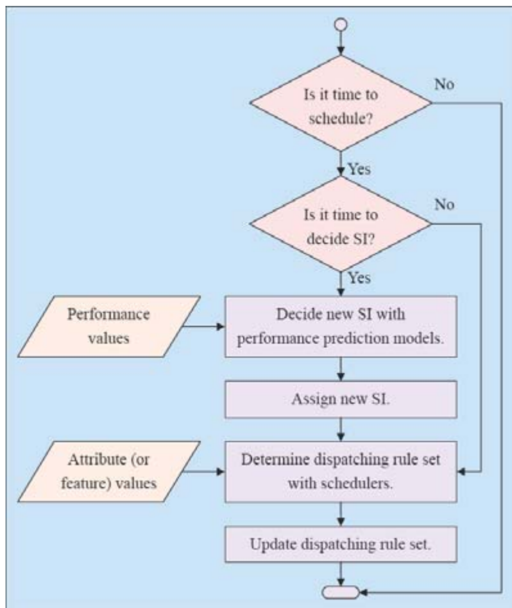


Figure 13 On-line rescheduling mechanism

**Procedure of Training SVM Classification Model**

The overall procedure of training SVM classification model is shown in Figure 14. After a long run of simulation, each attribute value of every intrabay is collected. Traditional scheduling methods make decisions based on the explicit system attributes directly, such as machine utilizations, job tardiness, etc. In summary, six local attributes for the intrabay and one global attribute for the fab are chosen as follows: the mean utilization of the machines in the intrabay, the number of the jobs in the intrabay, the mean sojourn time of the jobs in the intrabay, the mean remaining processing time of the jobs in the intrabay, the mean slack time of the jobs in the intrabay, the mean tardiness time of the jobs in the intrabay, and the level of machine breakdown in the fab.

In order to deploy different dispatching rules to different intrabays, k-Means is used for clustering the intrabays of the fab. In particular, the reason for clustering is to reduce the search space and simulation time. That is, if there are 23 intrabays in the fab and these intrabays are clustered to 5 clusters, and then the search space is reduced from $7^{23}$ ($2.737\times10^{19}$) to $7^5$ ($1.6807\times10^4$).

Then GA is employed for searching dispatching rule sets which promote better performance. With attributes as the system conditions corresponding to dispatching rules, the SVM classifier is constructed as the scheduler. The dispatching rules used in this paper are selected from previous researches and described in Table 2.

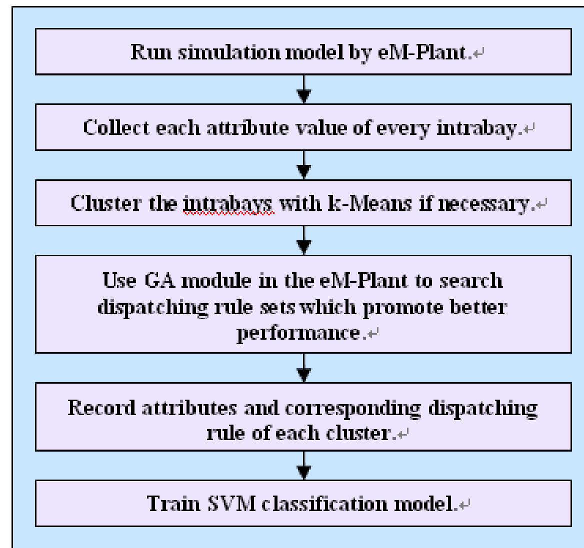


Figure 14 Procedure of training SVM classification model.

Table 2. Dispatching rules

| Dispatching Rule | Description | Criterion |
|---|---|---|
| FIFO | First In First Out | First in first out |
| SPT | Shortest Processing Time | Shortest processing time first |
| TIS | Time In System | Longest one first |
| SRPT | Shortest Remaining Processing Time | Shortest RPT first |
| CR | Critical Ratio | Smallest one first |
| LS | Least Slack | Smallest slack time first |
| EDD | Earliest Due Date | Earliest due date first |

**Procedure of Building ANFIS Prediction Model**

The entire procedure for building ANFIS prediction model is shown in Figure 15. After observation of a long run simulation, the period between two decision points is set as 12 days. Between two decision points, the length of the scheduling intervals (SI) may be 1 day, 2 days, 3 days, 4 days, 6 days or 12 days. For example, if SI is 2 days, scheduling will be taken six times between these two decision points. A sketch map is shown in Figure 16.

For the sake of on-line deciding the scheduling intervals between two decision points, six ANFIS prediction models are built, as shown in Figure 15. Performance values of previous four-time scheduling are fed as the prediction model's input, and then the performance of following 12-day scheduling result is predicted. Predicted performance values of six ANFIS prediction models are compared to decide the actual scheduling intervals between these two decision points.

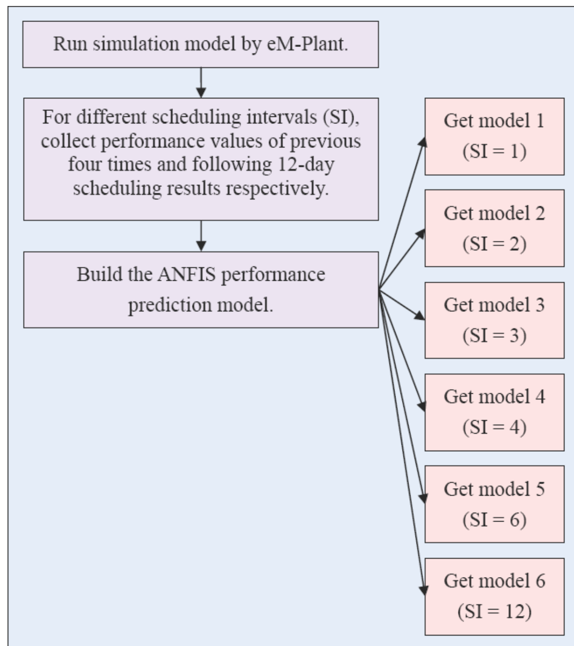


Figure 15 Procedure of building ANFIS prediction model

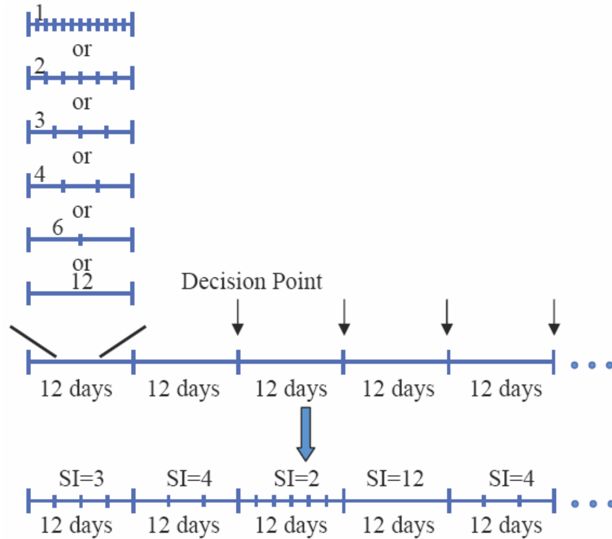


Figure 16 Sketch map of interval variant rescheduling

### 3.3.2 Accomplishment 2: Decision Support System

This section is devoted to the proposed method for knowledge extraction, learning, and update. Right after that is the implementation of the overall decision support system.

**Knowledge Extraction, Learning, and Update**

Whereas data are a collection of facts, measurements, and statistics, information is organized or processed data that are timely and accurate. The information extracted here contains throughput, WIP, each product's mean flow time, tardy number, intrabay attributes, tool parameters, job conditions, etc. Then some information can be extracted to knowledge.

The overall procedure for knowledge extraction, learning, and update is shown in Figure 17. The first step is to reduce the amount of information and to get the representative information so that the size of built decision tree will be kept and small. Then, utilize the representative information to build decision tree or GDA-based decision tree. The reason for building decision tree is that it is easy to transform it to rules as knowledge. And GDA-based decision tree is used to enhance the accuracy rate. When accumulating a certain amount of information, use k-means to update the representative information. The updated representative information is taken to build a new decision tree, so the accuracy rate will not be down.

The information here is extracted from the SEMATECH Model's system attributes. Figure 18 shows the position of representative information with update, and it can be seen that the representative information is only be fine tuned. It can be observed that the circled nodes' attributes are almost the same with update and theirs cut values are only be fine tuned. For the un-circled nodes, they may be new nodes or will be automatically pruned with update. Figure 19 shows the accuracy rate of knowledge with update and Figure 20 reveals the structural complexity of knowledge with update.

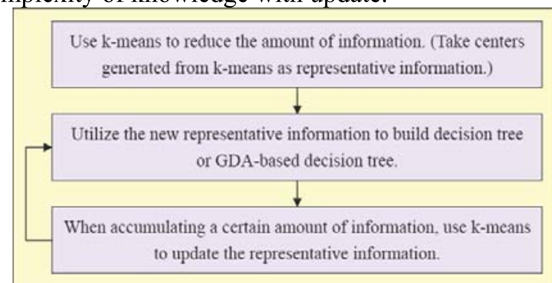


Figure 17 Procedure for knowledge extraction, learning, and update

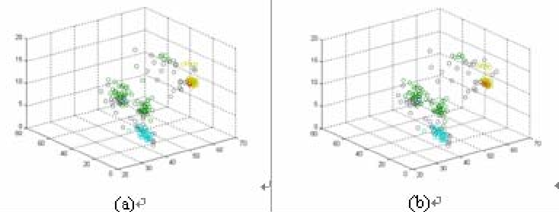


Figure 18 Position of representative information with update

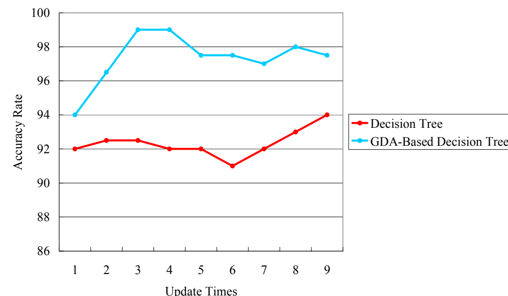


Figure 19 Accuracy rate of knowledge with update

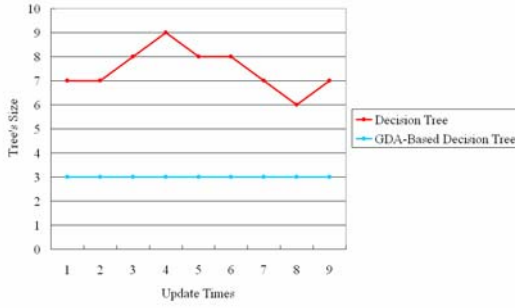


Figure 20 Structural complexity of knowledge with update

**Decision Scenarios**

Four scenarios are provided to support decision making. The first offers decision makers to decide product mix ratio with the concept of TOC. One key idea of TOC is that the system's constraints (also called bottleneck resources or capacity constraint resources, CCRs) determine the system's performance and should be the focus of management attention. In order to acquire the highest profit attainable, the CCR must be fully utilized. TOC approach decides the product type and the corresponding quantity to produce a given market potential.

The second scenario can control job arrival rate through the monitoring of WIP. And then the third one supplies to decide dispatching rules in terms of the knowledge extracted from the method proposed in section A. The last scenario aids preventive maintenance with the information of each machine's PM schedule. All these scenarios are through web pages to achieve knowledge sharing.

### 3.4 Subproject 4: Monitoring and Control of Semiconductor Supply Chains with RFID-based Information

#### 3.4.1 Accomplishment 1：Construct a forward echelon-based monitoring model

The proposed scheme is to construct a forward two-echelon model with the goal of minimizing the echelon WIP inventory control limits under a target service level. The echelon WIP concept is different from the traditional stage inventory. In the traditional stage view, the WIP is monitored and controlled in each stage. However, echelon view considers all WIP inventory from the certain stage to the final stage. Their relationship is shown in Figure 21.

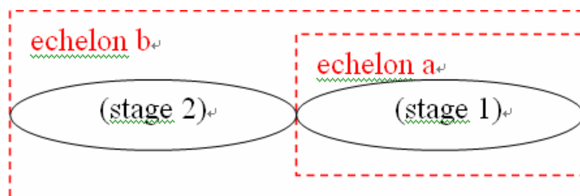


Figure 21 Definitions of stage and backward echelon inventory

However, most of the echelon inventory control has been focused on the logistics and distribution systems, in which lead time is usually fixed without considering of characters of production and different power of each member. In addition, the echelon is usually counted backward as shown in Figure 21. These assumptions might not be applicable under a semiconductor supply chain, in which lead time is dependent on the factory loadings and the control power is usually stronger in the front stage (fab). As a result, the first task of this research is to extend the backward echelon-based inventory control method to a forward echelon-based inventory concept considering the dynamic lead time effect. The schematic of forward echelon inventory and stage inventory is shown in Figure 22.

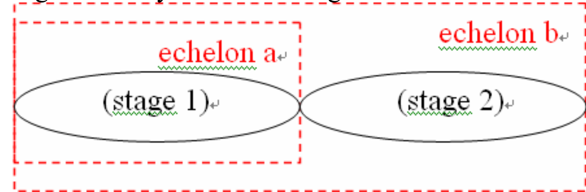


Figure 22 Definitions of stage and forward echelon inventory

Index

$t$: Time index

$n$: Stage index of each production

$m$: Echelon index

Input variables

$D_t$ : The demands in the period $t$ and follow $D_t \sim N(\mu, \sigma^2)$

$\theta_1$: The correlation coefficient of $D_t$ and $D_{t+1}$

$X_n$: The variable that presents the sum of demands which stage $n$ needs to satisfy in the future production lead time

$\rho$: The correlation coefficient of $X_1, X_2$

$l_n$: The production lead time of stage $n$

$B$: The expected number of blocking parts

$\alpha$: Service level $\alpha$ is defined as the fraction of periods that demands can be totally satisfied when the WIP is below the monitor limit

$\gamma$: Service level $\gamma$ is defined as the fraction of average cumulative backorders in the system divided by average current demand

Decision variables

$\bar{Z}_m$: The standardized $S_m$ on the basis of $X_2$

Other symbols

$ST_n$: The WIP inventory limit of stage $n$

$S_m$: The WIP inventory limit of echelon m form the echelon view

$\bar{S}_m$: The WIP inventory limit of echelon $m$ form the results of stage view

$M$: $\dfrac{\mu}{Var^{1/2}(X_2)}$

$V$: $\dfrac{Var^{1/2}(X_1)}{Var^{1/2}(X_2)}$

$A$: The algebras for from $\rho, V$

$\psi(\cdot,\cdot;\zeta)$ :The cumulative density function of the standardized bivariate normal with the

correlation coefficient $\zeta$

$\phi(\cdot)$: The probability density function of standardized normal

$\Phi(\cdot)$: The cumulative density function of standardized normal

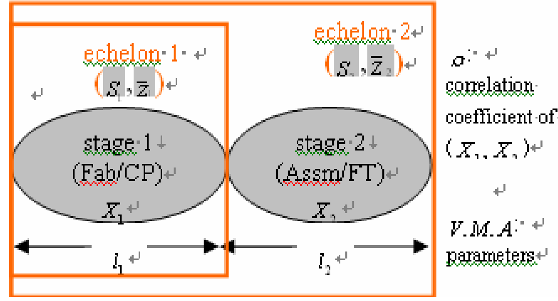


Figure 23 Parameters of the model

Forward two-echelon monitoring model

***Minimize***

$\overline{Z}_2$

***Subject to***

$$\alpha \le \psi\left(\frac{f(\overline{Z}_1)}{V}, \frac{f(\overline{Z}_2)}{\sqrt{A}}; \frac{\rho+V}{\sqrt{A}}\right)$$

$$(1-\gamma)M \ge \sqrt{A}\cdot\phi\left(\frac{f(\overline{Z}_2)}{\sqrt{A}}\right) - f(\overline{Z}_2)\cdot\left\{1-\Phi\left(\frac{f(\overline{Z}_2)}{\sqrt{A}}\right)\right\}$$

$$-f(\overline{Z}_1)\cdot\left(\Phi\left(\frac{f(\overline{Z}_2)}{\sqrt{A}}\right)-\alpha\right)$$

$$+V\phi\left(\frac{f(\overline{Z}_1)}{V}\right)\cdot\Phi\left(\frac{V\cdot f(\overline{Z}_2)-(\rho+V)\cdot f(\overline{Z}_1)}{V\sqrt{1-\rho^2}}\right)$$

$$-V\left(\frac{\rho+V}{\sqrt{A}}\right)\cdot\phi\left(\frac{f(\overline{Z}_2)}{\sqrt{A}}\right)\left\{1-\Phi\left(\frac{A\cdot f(\overline{Z}_1)-V\cdot(\rho+V)\cdot f(\overline{Z}_1)}{V\cdot\sqrt{A}\cdot\sqrt{1-\rho^2}}\right)\right\}$$

$$\overline{Z}_1 \le \overline{Z}_2 + l_2\cdot M$$

Where,

$$f(\overline{Z}_1) = \overline{Z}_1 - B - \left(1-\Phi\left(\frac{\overline{Z}_1}{V}\right)\right)\times\overline{Z}_1\times\frac{1}{8}erfc\left(\frac{\Phi^{-1}(\alpha_c)}{\sqrt{2}}\right)^2$$

$$f(\overline{Z}_2) = \overline{Z}_2 - B - \left(1-\Phi\left(\frac{\overline{Z}_2}{\sqrt{A}}\right)\right)\times\overline{Z}_2\times\frac{1}{8}erfc\left(\frac{\Phi^{-1}(\alpha_c)}{\sqrt{2}}\right)^2$$

$$\overline{Z}_1 = \frac{S_1-(l_1)\mu}{Var^{1/2}(X_2)},\quad \overline{Z}_2 = \frac{S_2-(l_1+l_2)\mu}{Var^{1/2}(X_2)}$$

$$V = \frac{Var^{1/2}(X_1)}{Var^{1/2}(X_2)},\quad M = \frac{\mu}{Var^{1/2}(X_2)}$$

$$A = V^2 + 2\rho\cdot V + 1$$

$$B = V\cdot\phi\left(\frac{\overline{Z}_1}{V}\right)\cdot\left\{\Phi\left(\frac{\overline{Z}_2-\left(1+\frac{\rho}{V}\right)\cdot\overline{Z}_1}{\sqrt{1-\rho^2}}\right)\right\}$$

$$+\phi(\overline{Z}_2-\overline{Z}_1)\cdot\left\{1-\Phi\left(\frac{(1+\rho V)\overline{Z}_1-(\rho V)\cdot\overline{Z}_2}{V\sqrt{1-\rho^2}}\right)\right\}$$

$$+\sqrt{A}\cdot\phi\left(\frac{\overline{Z}_2}{\sqrt{A}}\right)\cdot\left\{1-\Phi\left(\frac{\frac{(\rho+V)\cdot V\overline{Z}_2}{\sqrt{A}}-\sqrt{A}\cdot\overline{Z}_1}{V\sqrt{1-\rho^2}}\right)\right\}$$

$$-\overline{Z}_1\cdot\left[\Phi(\overline{Z}_2-\overline{Z}_1)-\psi\left(\overline{Z}_2-\overline{Z}_1,\frac{\overline{Z}_1}{V},\rho\right)\right]$$

$$-\overline{Z}_2\cdot\left[1-\alpha-\Phi(\overline{Z}_2-\overline{Z}_1)+\psi\left(\overline{Z}_2-\overline{Z}_1,\frac{\overline{Z}_1}{V},\rho\right)\right]$$

In order to bring the feature of the production system into the model, the model is modified as follows:

(1) In order to take the relationship, the cycle time of each echelon should be estimated in the form of

$$\begin{cases} N(\alpha_1+\beta_1 x_i,\ a_1+b_1 x_i) & \text{if } x_i \le \omega \\ N(\alpha_2+(\beta_1+\beta_2)x_i,\ a_2+(b_1+b_2)x_i) & \text{otherwise} \end{cases},$$

which is the relationship of WIP and cycle time from production view. Next, the relationship of production lead time and WIP given the service level requirement is estimated in the form of $l\cdot\mu_D+\phi^{-1}(\alpha)\cdot\sqrt{l}\cdot\sigma_D$ and this is the demand view of the relationship. Therefore, the proper lead time is estimated by solving the equation simultaneously.

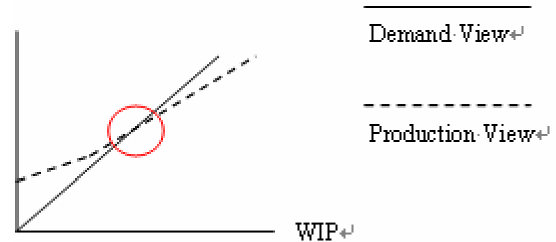


Figure 24 production lead time estimation

(2) The WIP is blocked and the cycle time might exceed the lead time when the WIP level reaches a monitoring limit. Thus, the effects are estimated by the reduction part from $\overline{Z}_m$. $1-\Phi(Z_n)$ part estimates the probability that WIP level exceeds monitoring limit, $Max\{X_1-S_1, X_1+X_2-S_2, 0\}$ part estimates the blocked WIP that would enter in the next period, and $Z_n\frac{1}{8}erfc\left(\frac{l'}{\sqrt{2}}\right)^2$ part estimates the WIP remain in the system due to longer cycle time.

### 3.4.2 Accomplishment 2 : Develop CONWIP control method and solution procedures

To reduce overall WIP control limit, the

service level of smaller echelon is set higher than the overall required service level. This is due to the fact that production time of the front-end member is loner than that of downstream stage in semiconductor supply chain. Therefore, setting higher internal service level results in a lower blocking probability and minimizes overall WIP. Consequently, lower WIP monitoring limits can be obtained by setting higher service level However, the increase of service level of smaller echelons would not only result in the increase of WIP monitoring limits but also the cycle times.

In solving the forward two-echelon control model, the following heuristic is adapted:

Step 1: solve the equation

$$\begin{cases} l\cdot\mu_D+\phi^{-1}(\alpha)\cdot\sqrt{l}\cdot\sigma_D= \\ \alpha_1+\beta_1 x_i+\phi^{-1}(\alpha_c)\sqrt{a_1+b_1 x_i} & \text{if } x_i\le\omega \\ l\cdot\mu_D+\phi^{-1}(\alpha)\cdot\sqrt{l}\cdot\sigma_D= \\ \alpha_2+(\beta_1+\beta_2)x_i+\phi^{-1}(\alpha_c)\sqrt{a_2+(b_1+b_2)x_i} & \text{otherwise} \end{cases}$$

for each echelon to obtain the initial lead time as model input.

Step 2: solve $\gamma$ constraint by setting $\overline{Z}_1=\Phi(\alpha)\cdot V$ as initial value. Then, increase $\overline{Z}_1$ and calculate the contribution. If $\overline{Z}_1\ge 3.5\cdot V$, set $\overline{Z}_1=3.5\cdot V$ and then solve the equation again to obtain the new $\overline{Z}_2$. If contribution less than $\varepsilon$, then stop increasing the $\overline{Z}_1$.

Step 3: use the result from step 2 to check if the $\alpha$ constraint is satisfied. If $\alpha$ constraint is satisfied, go to Step 4. Else, solve $\alpha$ constraint to obtain $\overline{Z}_2$ with fixed $\overline{Z}_1$.

Step 4: Calculate the WIP monitoring limit ($S_m$) from the standardized limit. Check the corresponding cycle times by the following equation for each echelon.

$$\begin{cases} N(\alpha_1+\beta_1 x_i,\, a_1+b_1 x_i) & \text{if } x_i\le\omega \\ N(\alpha_2+(\beta_1+\beta_2)x_i,\, a_2+(b_1+b_2)x_i) & \text{otherwise} \end{cases}$$

If the corresponding cycle time (production view) is smaller than the lead time (demand view) in the model, the WIP monitoring limit is obtained. Otherwise, the corresponding cycle time of echelon exceeds the lead time, increase the lead time by one and go to step 1.

### 3.4.3 Accomplishment 3：Design scenarios and conduct simulations to compare the performance of different control schemes

A simulation model is built according to the assumptions of the model. Next, simulations are performed with both monitoring and control schemes together. The CONWIP control rule is adopted in which a lot can't be released whenever either stage or echelon inventory limits are reached. The WIP monitoring limits for simulations are shown in Table 3 and results of the simulation are shown in Table 4.

Table 3. Analytical WIP inventory limits

| Settings | $D_t\sim N(497.556,112.2^2)$; $l_1=36, l_2=11$; $\alpha\ge 0.9$ | | | |
|---|---|---|---|---|
| | $ST_1$ | $ST_2$ | $S_1$ | $S_2$ |
| Stage Based | 18775 (100%) | 5951 (100%) | 18775 (100%) | 24726 (100%) |
| Forward Echelon Based | 19421 (103.44%) | 5109 (85.85%) | 19421 (103.44%) | 24530 (99.2%) |
| Echelon Based | 6184 (103.92%) | 18284 (97.39%) | 6184 (103.92%) | 24468 (98.96%) |

Table 4. Simulation performance results

| | Forward-Echelon | | | Stage | |
|---|---|---|---|---|---|
| Echelon | WIP | Planned lead time | Stage | WIP | Planned lead time |
| 1 | 19421 | 36 | 1 | 18775 | 36 |
| 2 | 24530 | 47 | 2 | 5971 | 11 |
| Total WIP | 24530 | 47 | Total WIP | 24726 | 47 |
| Service level | alpha service level | gamma service level | Service level | alpha service level | gamma service level |
| Mean | 0.91121 | 0.94657 | Mean | 0.79023 | 0.89245 |
| Std. | 0.04424 | 0.03608 | Std. | 0.05756 | 0.04911 |

As shown in Table 4, with a lower supply chain inventory, the proposed forward two-echelon inventory monitoring and control method can achieve a higher service level than the stage-based inventory monitoring and control method. This result is due to the fact that the control and monitoring based on forward echelon inventory utilizes the global information of the whole supply chain while the traditional method uses only local information to control and monitor. A careful study of the simulation results further confirm that stage 1's inventory in the forward two-echelon model has a higher inventory position and results in a lower blocking probability. This is the idea of increasing the internal service level to lower the overall WIP monitoring limit.

## 四、參考文獻


[1] N. Bahaji and M. E. Kuhl, “A Simulation Study of Composite Dispatching Rules, CONWIP and Push Lot Release in Semiconductor Fabrication,” *International Journal of Production Research,* submitted for publication.

[2] G. Baudat and F. Anouar, “Generalized Discriminant Analysis using a Kernel Approach,” *Neural Computation*, Vol. 12, No. 10, pp. 2385-2404, Jan. 2000.

[3] E. Campbell and J. Ammenheuser, “300 mm Factory Layout and Material Handling Modeling: Phase II Report,” *International SEMATECH Technology Transfer Document,* No. 99113848B-ENG, 2000.

[4] S. H. Chung, H. I. Lee, and W. L. Pearn, “Product Mix Optimization for Semiconductor Manufacturing Based on AHP and ANP Analysis,” *International Journal of Advanced Manufacturing Technology,* Vol. 25, No. 11, pp. 1144-1156, Jun. 2005.

[5] C. Cortes and V. Vapnik, “Support-Vector Networks,” *Machine Learning,* Vol. 20, No. 3, pp. 273-297, Sep. 1995.

[6] R. O. Duda, P. E. Hart, and D. G. Stork, *Pattern Classification,* 2nd Edition, New York: Wiley, pp. 526-528, 2000.

[7] T. C. Hsu and S. H. Chung, “The TOC-Based Algorithm for Solving Product Mix Problems,” *Production Planning and Control,* Vol. 9, No. 1, pp. 36-46, Jan. 1998.

[8] C. W. Hsu and C. J. Lin, “A Comparison of Methods for Multi-Class Support Vector Machines,” *IEEE Transactions on Neural Networks,* Vol. 13, No. 2, pp. 415-425, Mar. 2002.

[9] S. R. Jang, “ANFIS: Adaptive-Network-Based Fuzzy Inference System,” *IEEE Transactions on Systems, Man and Cybernetics,* Vol. 23, No. 3, pp. 665-685, Jun. 1993.

[10] S. R. Jang, C. T. Sun, and E. Mizutani, *Neuro-Fuzzy and Soft Computing,* 1st Edition, New Jersey: Prentice-Hall, pp. 175-180, 1997.

[11] R. T. Marler and J. S. Arora, “Survey of Multi-Objective Optimization Methods for Engineering,” *Structural and Multidisciplinary Optimization,* Vol. 26, No. 6, pp. 369-395, Apr. 2004.

[12] H. S. Min and Y. Yih, “Selection of Dispatching Rules on Multiple Dispatching Decision Points in Real Time Schedule of Semiconductor Wafer Fabrication Systems,” *International Journal of Production Research,* Vol. 41, No. 16, pp. 3921-3941, Nov. 2003.

[13] R. Rangsaritratsamee, W. G. Ferrell, and M. B. Kurz, “Dynamic Rescheduling that Simultaneously Considers Efficiency and Stability,” *Computers and Industrial Engineering,* Vol. 46, No. 1, pp. 1-15, Mar. 2004.

[14] C. R. Tsai, “Development of a Real-Time Scheduling and Rescheduling System Based on RFID for Semiconductor Foundry Fabs,” *Master Thesis,* Graduate Institute of Industrial Engineering, National Taiwan University, 2005.

[15] R. Uzsoy, C. Y. Lee, and L. A. Matrin-Vega, “A Review of Production Planning and Scheduling Models in Semiconductor Industry, Part 1: System Characteristics, Performance Evaluation and Production Planning,” *IIE Transactions on Scheduling and Logistics,* Vol. 24, No. 4, pp. 47-59, 1992.

[16] V. Vapnik, *Statistical Learning Theory,* 1st Edition, New York: Wiley, 1998.

[17] G. E. Vieira, J. W. Herrmann, and E. Lin, “Analytical Models to Predict the Performance of a Single-Machine System Under Periodic and Event-Driven Rescheduling Strategies,” *International Journal of Production Research,* Vol. 38, No. 8, pp. 1899-1915, May 2000.

[18] CART: http://www.salford-systems.com/421.php

[19] Lagodimos, A.G., A. G. De Kok, and J. H. C. M. Verrijdt, “The robustness of multi-echelon service models under autocorrelated demands,” The Journal of the Operational Research Society, 46, 1, 92-103 (1995).

[20] Chen, C. Y. J., George E. I., and Tardif, V., “A Bayesian model of cycle time prediction,” IIE Transactions, 33, 921-930 (2001).